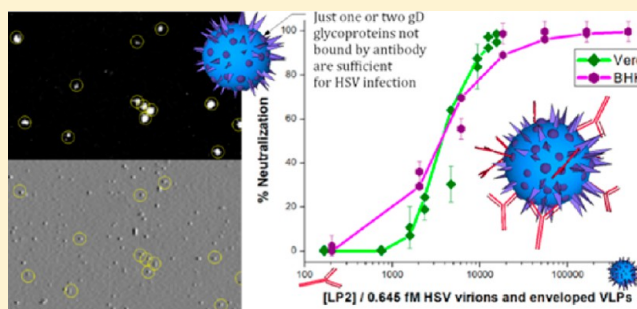


A Single gD Glycoprotein Can Mediate Infection by *Herpes simplex* VirusRichard W. Clarke,<sup>\*,†,‡</sup> Anna Drews,<sup>†,‡</sup> Helena Browne,<sup>§</sup> and David Klennerman<sup>\*,†</sup><sup>†</sup>Chemistry Department, University of Cambridge, Lensfield Road, Cambridge CB2 1EW, U.K.<sup>§</sup>Division of Virology, Pathology Department, University of Cambridge, Tennis Court Road, Cambridge CB2 1QP, U.K.

## S Supporting Information

**ABSTRACT:** *Herpes simplex* viruses display hundreds of gD glycoproteins, and yet their neutralization requires tens of thousands of antibodies per virion, leading us to ask whether a wild-type virion with just a single free gD is still infective. By quantitative analysis of fluorescently labeled virus particles and virus neutralization assays, we show that entry of a wild-type HSV virion to a cell does indeed require just one or two of the approximately 300 gD glycoproteins to be left unbound by monoclonal antibody. This indicates that HSV entry is an extraordinarily efficient process, functioning at the level of single molecular complexes.



## 1. INTRODUCTION

To accomplish membrane fusion, the *Herpes simplex* virus (HSV) envelope displays arrays of hundreds of copies of at least 12 glycoproteins. Of these, gD is essential for entry in combination with two other complexes, the trimer gB and the heterodimer gHgL.<sup>1–4</sup> One of the most potent monoclonal antibodies against gD is LP2.<sup>5</sup> However, neutralizing every virion in a suspension requires around 10 000 anti-gD LP2 antibodies per virion, a huge molar excess to the approximately 300 gD molecules, even though the LP2 antibody was always thought to bind gD strongly.<sup>5</sup> In this paper we reconcile these seemingly conflicting facts by carefully modeling the number of gD molecules expected to remain unbound by LP2, allowing us to fit neutralization curves by investigating how many free gD molecules are necessary for infection. This also requires careful characterization of two factors: the number of gD molecules per virion<sup>6</sup> and the proportions of different types of virus preparation particles (VPPs). The latter determination is necessary because, even in samples purified by density gradient centrifugation, most species present are not complete virions.<sup>7</sup> For example, virus-like particles (VLPs) are enveloped but lack a capsid. We determined the proportions of VPPs at a single-virion level using surface-scanning confocal fluorescence microscopy (SSCM).

The model we derive to fit neutralization curves of HSV by LP2 only has two remaining parameters, the avidity of the LP2 antibody for gD and the minimum infective number of free gD molecules on the virion envelope. This approach thus raises insights into the potency of LP2 and the efficiency of the viral glycoprotein in mediating entry.

## 2. METHODS, RESULTS, AND DISCUSSION

Using SSCM we made a study of fluorescently labeled virions on cultured neurons. This showed directly that the anti-gD antibody LP2 arrests HSV at the entry stage when in molar excess to the viral antigen. This entry requires gD to bind Nectin-1,<sup>8</sup> a cell adhesion molecule widely expressed on both human and murine neurons.<sup>8,9</sup> We expected to see LP2 block this interaction because HSV enters both Vero cells<sup>10</sup> and neuronal cell lines<sup>11,12</sup> at the plasma membrane without endocytosis and because the virus still adheres to surface glycosaminoglycans via gC and gB.<sup>13</sup> LP2 (as well as HD1, discussed below) belongs to group 1a of the anti-gD monoclonal antibodies,<sup>14,15</sup> which block entry without reducing virion adherence to the cell surface.<sup>16</sup> Thus, blocking many gD's is not expected to block HSV adhering to the cell, and we expect to be able to model the blocking of gD by LP2 independently of any effect on this adherence. Figure 1 shows the neutralizing capacity of LP2 in dual topographic/fluorescence scans of cultured neuronal cells exposed to HSV. At a molar ratio of 100:1 LP2 per VPP, almost all the virions still enter cells, whereas at a molar ratio of 1000:1 far fewer do. Plaque assays—capable of higher statistical accuracy than these demonstrative surface confocal scans—confirm that, even at a molar ratio of 1000:1, the neutralization is still not fully complete. This is illustrated in Figure 2A. The *x*-axis indicates that 64.5% of the 1 fM VPPs in the assay medium had envelopes, as detailed later in the text.

We suspected that full neutralization requires such high molar ratios because of high entry efficiency of gD in tandem with antibody dissociation at the extremely low virion titers

Received: April 17, 2013

Published: July 9, 2013

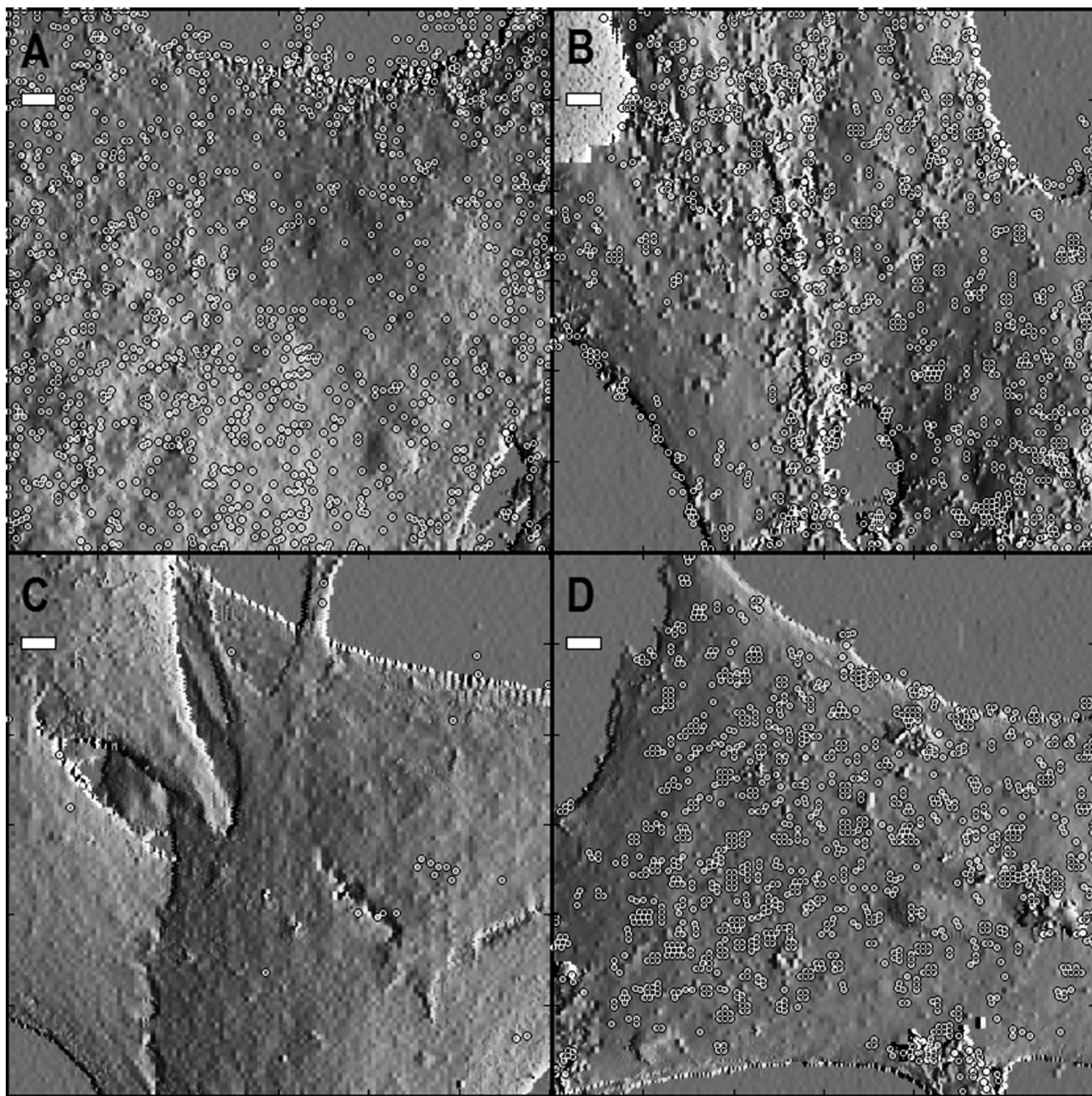


**Figure 1.** Virus preparation particles bound by LP2 anti-gD antibody on P4 cells. Upper (A,B) versus lower (C,D) panels: Fixed after incubation for 5 versus 65 min. Left-hand (A,C) versus right-hand (B,D) panels: At low (100) and high (1000) molar ratios of LP2 to VPP concentration. The neurons, shown in shadowed topography with  $2\ \mu\text{m}$  scale bars, are around  $15\ \mu\text{m}$  high. The VPPs, identified by fluorescence, are indicated by circles. There are far fewer fluorescent puncta at the low LP2 ratio after longer incubation: most of these particles entered the cells. With the high ratio of LP2, this decrease is not seen, verifying that very high molar ratios of LP2 arrest the infection cycle of HSV at the entry stage. The overwhelming absence of fluorescent puncta with low antibody, long incubation also indicates tegument and capsid are not required for entry, and the persistence of fluorescent puncta with high antibody indicates no alternative endocytosis of neutralized particles. Total frequencies from a sequence of such scans are shown in Figure S1. Neurons are infected by HSV natively but do not form the stable confluent layers required for plaque assays, so these scans are an important visualization of our main conclusions drawn from plaque-assayed neutralizations.

required for practical counting of plaques. Correct interpretation of HSV neutralization by LP2 therefore involves determining the minimum infective number of free gD molecules as well as the avidity of gD for LP2.

Using  $\lambda$  to denote the average expected number of gD molecules per viral envelope left unbound by LP2 IgG, the fraction of virions entirely capped by LP2 will be  $\exp(-\lambda)$

according to a Poisson distribution. Thus, if all gD antigens have to be capped by LP2 for the virion to be neutralized, we expect the neutralized fraction of virions to be  $\exp(-\lambda)$ . If a virion is still effectively neutralized when it has  $N$  free gD antigens, we can incorporate this into the model by summing the  $N$  successive terms of the Poisson distribution, up to  $(\lambda^N/N!) \exp(-\lambda)$ . For example, if a virion requires two or more free



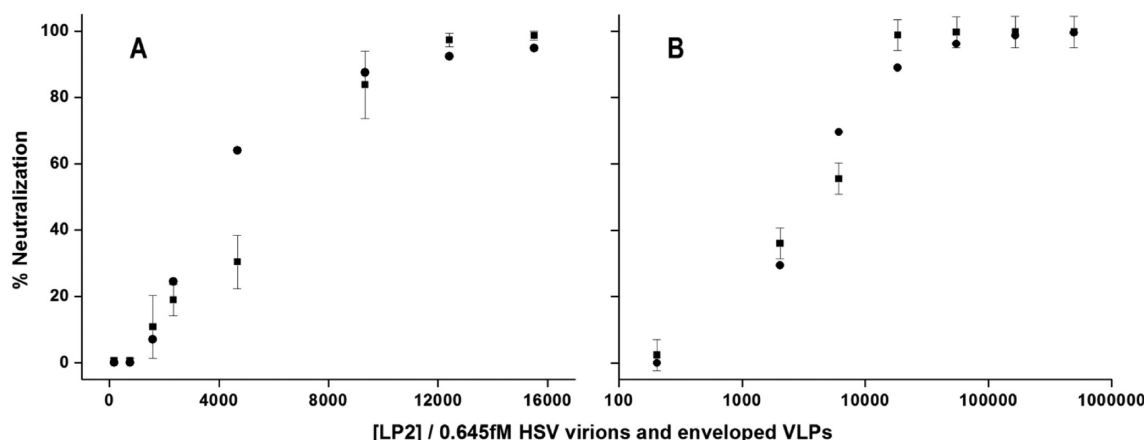


**Figure 2.** Neutralization of HSV by LP2 IgG. (A) Assay on Vero cells. The experimental data are indicated by squares. The circles correspond to the model described in the main text,  $100\%(1 + \lambda) \exp(-\lambda)$ , that assumes just two free gD antigens per virion are sufficient for that virion to enter a cell via an infective pathway. The only fitted parameter is the dissociation constant of gD and LP2, found to be 10.6 fM. (B) Assay on BHK cells. These experimental data are from Minson et al.<sup>5</sup> and are plotted with indicative error bars of 5%, the average Vero neutralization error. The circles correspond to the model described in the main text,  $100\% \exp(-\lambda)$ , that assumes just one free gD antigen per virion is sufficient for that virion to enter a cell via an infective pathway. The absolute concentration of LP2 IgG was not calibrated in the original reference, so it is scaled here to approximately match the Vero data. This means the  $K_D$  for this fit is not independent of the other value. The  $K_D$  is 4.0 fM.

gD antigens for entry, the model should include the terms for no free gD per virion plus the term for one free gD per virion:  $(1 + \lambda) \exp(-\lambda)$ . Three or more being required would be modeled by  $(1 + \lambda + (\lambda^2/2)) \exp(-\lambda)$ . If  $N$  approached the total number of gD molecules per virion, the distribution would be affected by this finite boundary, but as long as this is not the case, the model will be accurate.

The half-life of the dissociation of LP2 from gD is approximately 340 min according to the decay of Alexa-647 fluorescence shown in Figure S2. This is much shorter than the two days used for the plaque assays, so can we assume equilibrium conditions and write  $\lambda$  in terms of the dissociation constant,  $K_D = [gD][LP2]/[gD:LP2]$ , as follows:

$$\lambda = \frac{[gD]}{[VE]} = \frac{K_D[gD:LP2]}{[LP2][VE]}$$

In this equation  $[gD]$  is the concentration of free gD sites and  $[VE]$  is the concentration of viral envelopes in the virus preparation at the dilution used for the plaque assay, determined from the neutralization protocol and the confocal scan statistics below to be 0.645 fM, i.e.  $(60\% + 4.5\%) \times 10$  pM/10 000. However, the concentration of bound gD must be the difference between the concentrations of gD in total and in unbound form, and similarly the concentration of free LP2 is the amount not bound to gD. This allows us to form a quadratic equation for  $\lambda$  in terms of the molar ratio of LP2 to viral envelopes:

$$\lambda = \frac{K_D(X - \lambda)}{(R - (X - \lambda))[VE]}$$

$$\Rightarrow \lambda^2 + (R + K - X)\lambda - KX = 0$$

where  $X$  is the number of gD antigens per virion, around 335,  $R$  is the molar ratio of LP2 to the concentration of viral envelopes (the abscissae of the graphs), and we have made the substitution  $K = K_D/[VE]$ , equivalent to  $K = 1.55K_D/\text{fM}$ . Solving the equation then gives

$$\lambda = \left( \sqrt{(R + K - X)^2 + 4KX} - (R + K - X) \right) / 2$$

which completely determines  $\lambda$  as a function of the molar ratio, the number of antigens per virion, and the dissociation constant. Using this equation in the Poisson distribution formulas constitutes a realistic class of model for virus neutralizations. In order to make use of these formulas, the number of antigens per virion,  $X$ , must be found; three previous experimental protocols agree that there are approximately 335 gD glycoproteins per viral envelope.<sup>6</sup> To derive an accurate avidity, it only remains to properly calibrate the molar ratio  $R$  by measuring the actual proportion of virions and virion-like particles (VLPs) in the suspension that have envelopes. This proportion discounts particles of detritus as well as unenveloped capsid:tegument particles because neither of these types binds the antibody. We determined the frequencies of these different classes of particles from high-resolution SSCM measurements on glass by identifying non-overlapping local maxima of topography and fluorescence. A typical scan of an LP2-Alexa647-bound virion suspension is shown in Figure S3. The Alexa647 dye is far-red fluorescent, and the viral capsid protein VP26 was recombinantly labeled with Yellow Fluorescent Protein (yfp), which has previously been shown not to affect assembly or infectivity of the virus.<sup>17,18</sup> The total particle frequencies in four such scans were as follows: 4974 virions and VLPs with envelopes expressing gD, labeled via LP2-Alexa647; 1571 virions and capsid:tegument VLPs, labeled via VP26-yfp; 7727 topographic particles; and 350 virions, dual labeled by LP2-Alexa647 and VP26-yfp. These counts indicate that the particles in the virus preparation are  $16 \pm 0.6\%$  capsid:tegument particles without envelopes,  $60 \pm 1.2\%$  envelopes without capsids,  $4.5 \pm 0.2\%$  virions with envelopes and capsid:tegument, and  $19.5 \pm 1.3\%$  detritus. The value of 4.5% functional virions agrees with estimates from electron micrographs that the particle-to-plaque-forming unit ratio in HSV preparations purified from cell lysate by density gradient centrifugation is in the range 20:1 to 50:1, and generally about 20:1 for wild-type virions.<sup>7</sup>

Having done these calibrations, we were able to apply the model to the neutralization of HSV by LP2 on Vero cells: Both the data and fit are shown in Figure 2A. Only two parameters remain with which to fit the data, the number of free gD's

required for infection and the dissociation constant, so the fit is very good. High ratios of LP2 are required for full neutralization, far exceeding the number of gD binding sites. This is because the point at which almost all gD sites are capped is determined by the dissociation of the antibodies, which in these titrations only begins to become less significant at concentrations of around  $[1000 \text{ molar ratio} \times 10 \text{ pM VPP} / 10\,000 \text{ dilution}] = 1 \text{ pM}$  in the diluted assay medium. Thus, the model indicates that just two or more free gD antigens are sufficient for HSV to infect Vero cells and that the  $K_D$  for LP2:gD is 10.6 fM. This magnitude agrees with the original suspicion of very high avidity.

As a cross-check, we can use the literature to make an independent estimate of the LP2:gD dissociation constant. The epitope of LP2 likely includes the hotspots<sup>19–21</sup> in the binding regions on gD for both its main receptors Nectin-1 and HVEM. This is because these two binding regions on gD overlap<sup>22</sup> and the LP2 epitope is discontinuous,<sup>14,23</sup> which would correspond to LP2 binding both of these close but separate hotspots. The dissociation constants for gD:HVEM and gD:Nectin-1 have previously been determined by surface plasmon resonance of soluble truncated versions to be 3.2  $\mu\text{M}$ <sup>19,24,25</sup> and 17.1 nM,<sup>26</sup> respectively, although the affinity of gD for HVEM is likely enhanced by a factor of around 50<sup>19,24,25</sup> when the C-terminus moves away from the receptor binding region.<sup>14,22,27</sup> With the structurally reasonable assumption that the free energy difference between LP2 binding and dissociating is the sum of the free energies for HVEM and Nectin-1, this cross-check for the dissociation constant of LP2:gD yields 1–50 fM, in excellent agreement with the 10.6 fM value above.

The same class of model also fits two previous HSV neutralizations: by LP2 IgG assessed by plaque assay on BHK cells<sup>5</sup> and by another group 1a antibody,<sup>14</sup> HD1 IgG, assayed on CHO cells.<sup>15</sup> For the experiments carried out on Vero cells, the model for two or more free gD antigens was definitely necessary. In contrast, the model for just one or more free gD antigens mediating entry fitted the BHK data excellently, as shown in Figure 2B, and the fits for more free gD being necessary worsened progressively. This difference can be ascribed to the different cell lines. The model for just one or more free gD antigens mediating entry also fitted the HD1-CHO data excellently, as shown in Figure 3, and also fits the data for the other four antibodies assayed on CHO cells, shown in Figures S4–S7.

Overall, this study clearly indicates that for some cell lines just a single gD (along with gHgL and gB) can mediate infection. As shown in Figure 4, these results are robust to changes in the concentrations of the interactants by at least a factor of 2 either way, and are also stable to variation of the gD copy number over its wide range of biological variation,<sup>6</sup> 235–480. The fitted dissociation constants only change to 7.1 and 15.5 fM, respectively, well inside the expected range we calculated as a cross-check above. The same models work for different cell lines with different expression levels of receptors because the less specific interactions of viral glycoproteins like gC allow the virus to roll around on the cell surface while still remaining bound at a large number of weak binding sites. This maintains equilibrium with the antibody in solution and also allows any free gD molecules on the virus envelope to access any receptors on the cell surface.

In this way we find a 10.6 fM dissociation constant for LP2:gD and that just two free gD antigens per virion, likely functioning in complexes with the glycoproteins gHgL and gB,

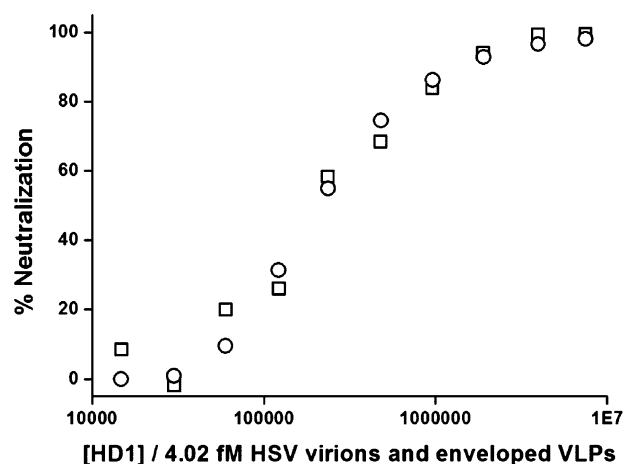


**Figure 3.** Neutralization of HSV by HD1 IgG, assayed on CHO cells. These experimental data are from Nicola et al.<sup>15</sup> The circles correspond to the model  $100\% \exp(-\lambda)$ , indicating that just one free gD antigen per virion is sufficient for infection. HD1 is group 1a like LP2.<sup>14</sup>

can mediate HSV entry for Vero cells, and one for BHK cells. This high entry efficiency agrees with the spheroidal geometry of HSV and with its widespread epidemiology despite limited modes of transmission.

It is worth highlighting that this result indicates LP2 has a discretized neutralization mechanism. Alternative neutralizing mechanisms would be lessening the general adhesion of HSV to cells or preventing the close approach of the two membranes, but these cannot account for the effectiveness of LP2. Our results show that LP2 molecules instead independently and completely block individual gD glycoproteins, which are essential to the virus's entry mechanism. This is why this antibody is so potent. As we have shown though, high molar ratios are still required because of dissociation at the very low concentrations required to conduct plaque assays.

### 3. CONCLUSIONS

We have shown that *Herpes simplex virus* (HSV) can still enter cells even if only one or two of approximately 300 gD glycoproteins on the virus surface are not bound by antibody. This is consistent with the findings of Huber et al.<sup>28</sup> and is an important result because it implies the HSV entry mechanism functions at the level of single complexes.

The fluorescence-based methods we present are generally applicable to other amorphous viruses, like influenza and human immunodeficiency virus, which cannot be adequately characterized by cryo-electron microscopy or X-ray diffraction for this purpose.

Also, for potentially neutralizing antibodies in general, we have shown that determining the relevant antigen copy number allows single-molecule-level information to be inferred from neutralization curves.

### 4. TECHNICAL METHODS

**4.1. Viruses.** The HSV-1 viruses used in this study were wild-type strain STH2 and a strain with Yellow-Fluorescent Protein (YFP)-tagged capsid (VP26-YFP)<sup>17,18</sup> called SCgH-VP26yfp. This strain was produced using the CR1 helper cell line trans-positive for gH.<sup>29</sup> The latter virus was used for all imaging experiments, as its phenotype is gH positive even though its genome lacks the gene for the entry-essential glycoprotein gH, allowing its use in category 1 containment

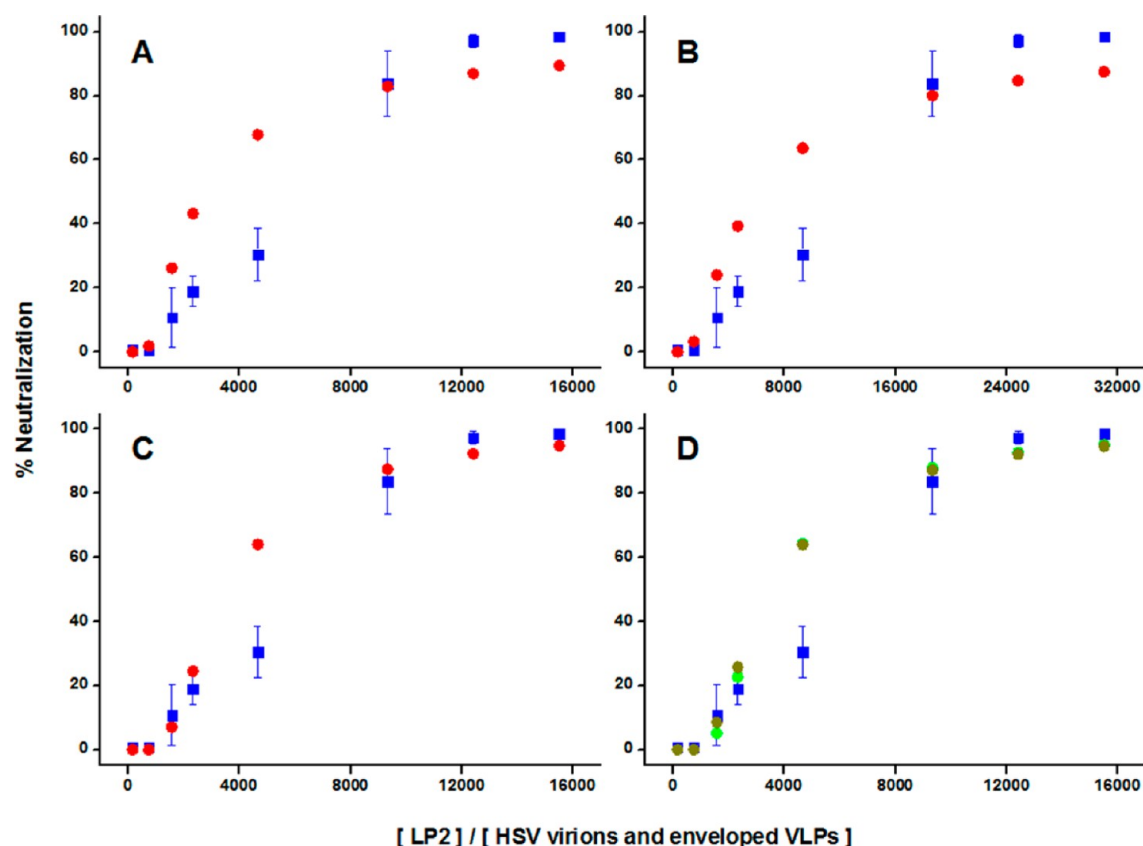


**Figure 4.** Illustration of fit stability to variation of virus concentration and gD copy number and dependence on number of gD molecules needed for infection. The data in these panels are from the plaque assays on Vero cells. The model for one or more gD being necessary (A,B) does not fit the data as well as that for two or more (C,D). Hypothetically raising, or lowering (B), the concentration of virus suspension by a factor of 2 hardly affects the shape of the function at all, and the dissociation constant only changes to 9.62 and 11.0 fM for hypothetical concentrations of twice and half of 0.645 fM, respectively. Similarly, hypothetically setting the gD copy number to the edges of its range (3), 488 and 235, rather than 335, does not change the shape of the function significantly either, as shown in (D). If very drastic changes were made to either of these pre-determined parameters, then the curves would no longer fit though—for example, increasing the gD copy number in the model to 8000 would result in the modeled neutralization curves rising too late. Overall we can conclude the fits are very stably sensitive to avidity and minimum infective number.

conditions. SCgH-VP26yfp was generated by co-infection with SCgH-pA<sup>30</sup> and SCVP26.<sup>18</sup> Fluorescent progeny which could only replicate on the CR1 helper cell line were identified and plaque-purified by limiting dilution on CR1 cells. Virions were then purified from supernatants of CR1 cells, and were therefore genotypically gH<sup>−</sup> but phenotypically gH<sup>+</sup>. Purified HSV1 virion preparations were made 2–3 days post-infection by successive centrifugation, filtration, and density gradient centrifugation according to the following procedure: The CR1 supernatant was clarified by centrifugation at 2500 rpm in a Mistral 6000 rotor (MSE UK Limited, London, United Kingdom) for 10 min. Virus particles were pelleted from the supernatant by centrifugation for 2 h at 16 000 rpm in a Beckman 19R rotor (Beckman, Fullerton, CA) at 4 °C. Pellets were re-suspended in 2 mL of phosphate-buffered saline (PBS) (NaCl, 150 mM; Na<sub>2</sub>HPO<sub>4</sub>, 10 mM; adjusted to pH 7.2), filtered by a 0.02 μm Anotop 25 mesh (Whatman International, Maidstone, England), sonicated, and layered onto 30 mL Ficoll gradients (5–15%) in PBS by centrifugation for 1.5 h at 12 000 rpm in a Beckman SW28 rotor at 4 °C. The visible band of virus at the center of the gradient was removed, diluted to 30 mL in PBS, and re-pelleted by centrifugation for 2 h at 20 000 rpm in a Beckman SW28 rotor. The resulting pellets were re-suspended in 500 μL of PBS and frozen at −70 °C in 50 μL aliquots. After purification, virus concentrations were estimated by comparison with counting negatively stained particles in an electron microscope as previously described.<sup>31</sup> The suspensions were stored in hydrophobic eppendorf tubes and handled with hydrophobic Gilson pipet tips, to which the particles do not bind due to their high charge density.

**4.2. Surface-Scanning Confocal Fluorescence.** Cell and slide surfaces were kept exactly in focus by tracking a nanopipet probe using scanning ion conductance microscopy. The microscope objective (Nikon, Plan Apo VC Water immersion ×60, MRD07601) was mounted in a piezoelectric drive (P-726, Physik Instrumente, UK) for this purpose, while the sample and nanopipet were positioned by XY (P-733.2DD) and Z (P-753) piezos, respectively. Nanopipets were fabricated using a Sutter Instrument Co. model P-2000 laser-based puller, pulling 10 cm length, 1 mm/0.50 mm outer/inner diameter fire-polished borosilicate glass capillaries with filaments (Sutter, via Intracel UK Ltd.) using the program Heat 350, Fil 3, Vel 30, Del 220, Pul, Heat 390, Fil 3, Vel 40, Del 180, Pul 255. The pull time range is 4.5–5.5 s. Typical nanopipet ion current was  $500 \pm 1.5$  pA for 200 mV electrode bias. Fluorescence photons were filtered by a dichroic mirror and longpass and bandpass filters before being detected by an avalanche photodiode and counted by a digital signal processor. Typical control set-point relative to maximum ion current was 99.2% (0.8% decrease relative to ion current in bulk solution).

**4.3. Measurements on Cultured P4 neuronal cells.** Quadruplicate samples of 11.2 μL of 10 pM suspensions of gH<sup>−</sup>/+ HSV VPPs were labeled with LP2-Alexa647 at molar ratios of 100:1 and 1000:1, and added to separate collagen-coated glass-bottom Petri dishes of P4 neuronal cells. The control dishes were fixed after waiting for 5 min for the suspensions to settle onto the cell surfaces by replacing the 2 mL buffer solution with 3.7% w/v methanol in PBS with 250 mM sucrose for 15 min before removing the fixing solution, washing twice with PBS, and adding L15 buffer for the surface scanning confocal measurement. The incubated dishes were fixed in



the same way after 1 h of incubation at 37 °C before fixation. PBS without divalent ions was used. An average of six 30  $\mu\text{m}$   $\times$  30  $\mu\text{m}$  scans were made per dish, and the red puncta were identified as local maxima exceeding a photon rate of 4 kHz not within four pixels (233 nm) of each other. The laser powers used in the experiment were 770 nW at 640 nm and 100 nW at 488 nm.

**4.4. Virus Neutralization Studies.** Purified wild-type HSV virions at a concentration of 10 pM VPPs were incubated with a range of dilutions of LP2-IgG in a total volume of 0.5 mL of PBS for 1 h at room temperature. The molar ratios of antibody to VPPs ranged from 0:1 (control) to 10 000:1. The amount of residual infectivity was determined by standard plaque assay on monolayers of Vero (African Green Monkey kidney) cells. The samples were diluted 1:10 000 before assaying infectivity and left for 2 days for plaques to form. The percentage of input infectivity that had been neutralized at each antibody concentration was then calculated relative to the controls with no antibody added. These assays were repeated twice, and the results represent the average titers obtained in two independent experiments.

## ■ ASSOCIATED CONTENT

### ■ Supporting Information

Supporting Materials and Methods (cell culture, fluorophore-labeled antibody, characterization of VPPs); supplementary results and figures. This material is available free of charge via the Internet at <http://pubs.acs.org>.

## ■ AUTHOR INFORMATION

### Corresponding Author

[rwc25@cam.ac.uk](mailto:rwc25@cam.ac.uk); [dk10012@cam.ac.uk](mailto:dk10012@cam.ac.uk)

### Author Contributions

<sup>‡</sup>R.W.C. and A.D. contributed equally.

### Notes

The authors declare no competing financial interest.

## ■ ACKNOWLEDGMENTS

This work was funded by a Milstein award from the MRC. We are grateful to S. Bell for performing plaque assays and cell culture, B. Bruun for purifying virus preparations, fluorescently labeling antibody, and cell culture, and C. Ironmonger for manufacturing components of the scanning microscope. R.W.C. thanks Christ's College, University of Cambridge, for a Research Fellowship.

## ■ REFERENCES

- (1) Cai, W. H.; Gu, B.; Person, S. J. *J. Virol.* **1988**, *62*, 2596.
- (2) Forrester, A.; Farrell, H.; Wilkinson, G.; Kaye, J.; Davis-Poynter, N.; Minson, T. J. *J. Virol.* **1992**, *66*, 341.
- (3) Ligas, M. W.; Johnson, D. C. *J. Virol.* **1988**, *62*, 1486.
- (4) Roop, C.; Hutchinson, L.; Johnson, D. C. *J. Virol.* **1993**, *67*, 2285.
- (5) Minson, A. C.; Hodgman, T. C.; Digard, P.; Hancock, D. C.; Bell, S. E.; Buckmaster, E. A. *J. Gen. Virol.* **1986**, *67*, 1001.
- (6) Clarke, R. W.; Monnier, N.; Li, H.; Zhou, D.; Browne, H.; Klenerman, D. *Biophys. J.* **2007**, *93*, 1329.
- (7) Döhner, K.; Radtke, K.; Schmidt, S.; Sodeik, B. *J. Virol.* **2006**, *80*, 8211.
- (8) Simpson, S. A.; Manchak, M. D.; Hager, E. J.; Krummenacher, C.; Whitbeck, J. C.; Levin, M. J.; Freed, C. R.; Wilcox, C. L.; Cohen, G. H.; Eisenberg, R. J.; Pizer, L. I. *J. Neurovirol.* **2005**, *11*, 208.
- (9) Shukla, D.; Scanlan, P. M.; Tiwari, V.; Sheth, V.; Clement, C.; Guzman-Hartman, G.; Dermody, T. S.; Valyi-Nagy, T. *Appl. Immunohistochem. Mol. Morphol.* **2006**, *14*, 341.
- (10) Milne, R. S. B.; Nicola, A. V.; Whitbeck, J. C.; Eisenberg, R. J.; Cohen, G. H. *J. Virol.* **2005**, *79*, 6655.
- (11) Lycke, E.; Hamark, B.; Johansson, M.; Krotochwil, A.; Lycke, J.; Svennerholm, B. *Arch. Virol.* **1988**, *101*, 87.
- (12) Nicola, A. V.; Hou, J.; Major, E. O.; Straus, S. E. *J. Virol.* **2005**, *79*, 7609.
- (13) Herold, B. C.; Visalli, R. J.; Susmarski, N.; Brandt, C. R.; Spear, P. G. *J. Gen. Virol.* **1994**, *75*, 1211.
- (14) Muggeridge, M. I.; Wu, T. T.; Johnson, D. C.; Glorioso, J. C.; Eisenberg, R. J.; Cohen, G. H. *Virology* **1990**, *174*, 375.
- (15) Nicola, A. V.; de Leon, M. P.; Xu, R.; Hou, W.; Whitbeck, J. C.; Krummenacher, C.; Montgomery, R. I.; Spear, P. G.; Eisenberg, R. J.; Cohen, G. H. *J. Virol.* **1998**, *72*, 3595.
- (16) Cohen, G. H.; Isola, V. J.; Kuhns, J.; Berman, P. W.; Eisenberg, R. J. *J. Virol.* **1986**, *60*, 157.
- (17) Desai, P.; Person, S. J. *J. Virol.* **1998**, *72*, 7563.
- (18) Hutchinson, L.; Whiteley, A.; Browne, H.; Elliott, G. *J. Virol.* **2002**, *76*, 10365.
- (19) Connolly, S. A.; Landsburg, D. J.; Carfi, A.; Wiley, D. C.; Eisenberg, R. J.; Cohen, G. H. *J. Virol.* **2002**, *76*, 10894.
- (20) Connolly, S. A.; Landsburg, D. J.; Carfi, A.; Whitbeck, J. C.; Zuo, Y.; Wiley, D. C.; Cohen, G. H.; Eisenberg, R. J. *J. Virol.* **2005**, *79*, 1282.
- (21) Bogan, A. A.; Thorn, K. S. *J. Mol. Biol.* **1998**, *280*, 1.
- (22) Di Giovine, P.; Settembre, E. C.; Bhargava, A. K.; Luftig, M. A.; Lou, H.; Cohen, G. H.; Eisenberg, R. J.; Krummenacher, C.; Carfi, A. *PLoS Pathog.* **2011**, *7*, e1002277.
- (23) Muggeridge, M. I.; Isola, V. J.; Byrn, R. A.; Tucker, T. J.; Minson, A. C.; Glorioso, J. C.; Cohen, G. H.; Eisenberg, R. J. *J. Virol.* **1988**, *62*, 3274.
- (24) Rux, A. H.; Willis, S. H.; Nicola, A. V.; Hou, W.; Peng, C.; Lou, H.; Cohen, G. H.; Eisenberg, R. J. *J. Virol.* **1998**, *72*, 7091.
- (25) Willis, S. H.; Rux, A. H.; Peng, C.; Whitbeck, J. C.; Nicola, A. V.; Lou, H.; Hou, W.; Salvador, L.; Eisenberg, R. J.; Cohen, G. H. *J. Virol.* **1998**, *72*, 5937.
- (26) Zhang, N.; Yan, J.; Lu, G.; Guo, Z.; Fan, Z.; Wang, J.; Shi, Y.; Qi, J.; Gao, G. F. *Nature Commun.* **2011**, *2*, 577.
- (27) Krummenacher, C.; Supekar, V. M.; Whitbeck, J. C.; Lazear, E.; Connolly, S. A.; Eisenberg, R. J.; Cohen, G. H.; Wiley, D. C.; Carfi, A. *EMBO J.* **2005**, *24*, 4144.
- (28) Huber, M. T.; Wisner, T. W.; Hegde, N. R.; Goldsmith, K. A.; Rauch, D. A.; Roller, R. J.; Krummenacher, C.; Eisenberg, R. J.; Cohen, G. H.; Johnson, D. C. *J. Virol.* **2001**, *75*, 10309.
- (29) Boursnell, M. E.; Entwisle, C.; Blakeley, D.; Roberts, C.; Duncan, I. A.; Chisholm, S. E.; Martin, G. M.; Jennings, R.; Ni Challanain, D.; Sobek, I.; Inglis, S. C.; McLean, C. S. *J. Infect. Dis.* **1997**, *175*, 16.
- (30) Harman, A.; Browne, H.; Minson, A. C. *J. Virol.* **2002**, *76*, 10708.
- (31) Watson, D. H.; Russel, W. C.; Wildy, P. *Virology* **1963**, *19*, 250.